Geomechanics and Engineering, *Vol. 20, No. 3 (2019) 221-232*
DOI: https://doi.org/10.12989/gae.2020.20.3.221

Effect of constant loading on unsaturated soil under water infiltration conditions

Ali Murtaza Rasool*[1,2] and Jiro Kuwano[2a]

[1]National Engineering Services Pakistan (NESPAK), Lahore, Pakistan
[2]Department of Civil & Environmental Engineering, Saitama University, 255 Shimo-Okubo, Sakur-ku, Saitama-shi, Saitama 338-8750, Japan

(Received April 4, 2019, Revised January 11, 2020, Accepted January 18, 2020)

Abstract. In many tropical regions, soil structures often fail under constant loads as a result of decreasing matric suction due to water infiltration. Most of the previous studies have been performed by infiltrating water in the soil specimen by keeping shear stress constant at 85-90% of peak shear strength in order to ensure specimen failure during water infiltration. However, not many studies are available to simulate the soil behavior when water is infiltrated at lower shear stress and how the deformations affect the soil behavior if the failure did not occur during water infiltration. This research aimed at understanding both the strength and deformation behavior of unsaturated soil during the course of water infiltration at 25%, 50% and 75% of maximum deviatoric stress and axial strain by keeping them constant. A unique stress-strain curve expresses the transient situation from unsaturated condition to failure state due to water infiltration is also drawn. The shearing-infiltration test results indicate that the water infiltration reduces matric suction and increase soil deformation. This research also indicates that unsaturated soil failure problems should not always be treated as shear strength problems but deformation should also be considered while addressing the problems related to unsaturated soils.

Keywords: triaxial test; water infiltration; matric suction; shear strength; deformation behavior

1. Introduction

Many geotechnical and geoenvironmental engineering structures such as natural or man-made slopes and embankments are generally in an unsaturated state. These structures often fail suddenly under constant loads as a result of decreasing matric suction due to water infiltration during natural events. The influence of natural events such as evaporation and rainfall results in groundwater table fluctuations (Pirone *et al.* 2015). Raising of the groundwater table due to rainfall influences the nature and behavior of the soil in response to the negative pore water (also known as suction). In many tropical regions, slope failures normally occur in shallow unsaturated zones having a deep groundwater table. Most of the year, such slopes remain in an unsaturated state with negative pore water pressure adding to the shear strength and stability of the slope. Infiltration of rainwater into the slope surface reduces matric suction, thereby, decreasing the shear strength of soil which ultimately leads to slope failure (Bishop 1960, Fredlund *et al.* 2012, Mahmood *et al.* 2016). It has been generally claimed that during rainfall the increased water content in the soil decreases the soil suction above the groundwater table, and thus the shear strength of the soil. Water infiltration can lower the shear strength to a value close to the average shear stress along the potential failure surface and consequently trigger a landslide. (Gui and Wu 2014). When the soil is subjected to water infiltration there will not only be reduction in shear strength of soil but deformation will also occur. The research by Nishigata *et al.* 2003 stated that the deformation of soil caused by water infiltration is also a very important factor. Even if the slope is not failed, significant deformation may hinder the function of soil structures. Therefore, when analyzing the stability of slopes, strength and deformation characteristics of unsaturated soil become important.

The pore water pressure changes and deformation characteristics of an unsaturated slope can be studied by conducting various types of laboratory tests. The data from laboratory tests can be obtained in a relatively short time as compared to full-scale tests. A reasonable estimation of pore-water pressure and deformation characteristics of soils during water infiltration can be made from laboratory tests. There are two alternatives for the laboratory tests. The first alternative is to conduct small-scale tests on an instrumented slope model. The second alternative is to perform water infiltration tests on a soil specimen inside a triaxial test apparatus. Kim and Jeong (2017) presented a case study and numerical investigation to study the hydro-mechanical response of a shallow landslide in unsaturated slope subjected to rainfall infiltration using a coupled model. The coupled model was verified against experimental data from the shearing-infiltration triaxial tests. It was found that the coupled model properly described progress failure of a slope on a highly transient condition. The triggering phase of rainfall-induced

*Corresponding author, Senior Engineer, Ph.D.
E-mail: ali.murtaza@nespak.com.pk,
ali_eng@hotmail.com
[a]Ph.D.
E-mail: jkuwano@mail.saitama-u.ac.jp

ISSN: 2005-307X (Print), 2092-6219 (Online)

landslides in coarse-grained soils was studied by Sorbino and Nicotera (2013) and observed that landslides are frequently related to rainfall events that significantly reduce matric suction in the shallower soil layers. Melinda *et al.* (2004) investigated the strength and deformation characteristics of a re-compacted residual soil during water infiltration using two modified direct shear apparatuses. They suggested that the slope failure was associated with the reduction of suction in the soil. To verify the volume change theory for unsaturated soil Meilani *et al.* (2005) conducted triaxial tests to study the pore-water pressure and water volume change of re-compacted coarse kaolin under water infiltration conditions. Gui & Wu (2014) studied the mechanical behavior and failure mechanism of residual soil under constant suction and water infiltration conditions. The shearing infiltration tests were conducted by keeping deviatoric stress constant at 76-85%. It was observed that excessive deformation and the eventual softening of soil are sometimes the main cause of water infiltration induced failure. Kim *et al.* (2018) showed the stress path followed by the soil specimens in consolidated drained (CD) triaxial test under a constant matric suction and in a water infiltration test under constant deviatoric stress and compared the test result with numerical analysis. A reasonably good agreement of deviator stress-axial strain relationship was obtained between the numerical analysis results and laboratory test. In order to guarantee failure, the tests in these studies were conducted at a very high shear stress level i.e. about 85–90% of the soil's shear strength. However, not many studies are available to simulate the soil behavior when water is infiltrated at lower shear stress and to describe how the deformations affect the soil behavior if the failure did not occur during water infiltration.

In view of the above, an experimental program is designed with an aim to investigate the effect of constant loading on unsaturated soil behavior under water infiltration conditions. The soil samples were first sheared to 25%, 50% and 75% of maximum deviatoric stress and axial strain after that water was infiltrated by keeping the loading constant on the soil samples. The influence of constant loading has been reported on water infiltration, volume change and shear strength. Finally, a stress-strain relation also called a unique stress-strain curve has been drawn and discussed. A unique stress-strain curve shows the common stress path followed by soil specimens after water infiltration.

2. Experimental facilities and methodology

2.1 Description of the soil

Test material used in this study comprised of DL Clay, which is the commercial name of the soil. It is a non-plastic silt with a grain-size distribution as shown in Fig. 1. The silty soil has a relatively uniform grain size distribution with a median grain size D50 of approximately 0.03 mm. The appearance of freshly and freely deposited DL clay looks yellowish brown. Dried and powdered DL clay consists of Kaolinite and silica. Kaolinite and silica stones are used as agricultural chemicals. According to the Unified Soil Classification System (USCS), it is classified as silt and clay with low plasticity (ML-CL) and is composed of 90% silt and 10% clay which shows that it is larger in grain size than average clay. The reason for using DL clay is to overcome testing equipment limitations. DL clay has lower initial suction than that of kaolin clay under the same degree of saturation. Fig.2 shows that the maximum matric suction of studied soil is 50 kPa which is less than air entry value of membrane filter (AEV = 250 kPa) used in this study. The physical properties of DL Clay are summarized in Table 1.

Table 1 Physical properties of DL clay

Properties	Unit	Value
Density of soil particle, ρ_s	g/cm^3	2.654
Consistency	-	NP
Maximum dry density, ρ_{dmax}	g/cm^3	1.538
Optimum water content, OWC	%	21.5
Maximum particle size, d_{max}	mm	0.039
Coefficient of water permeability, k_s	m/s	6.68 x 10^{-7}

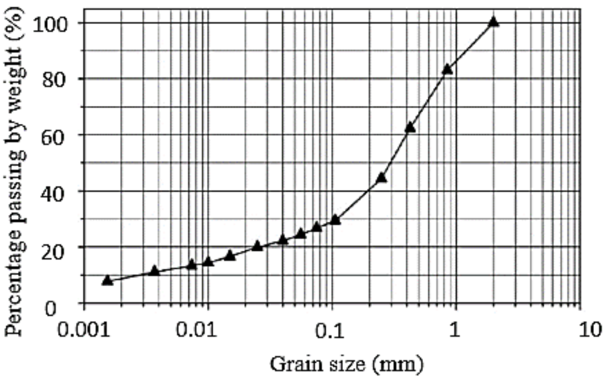

Fig. 1 Grain size accumulation curve

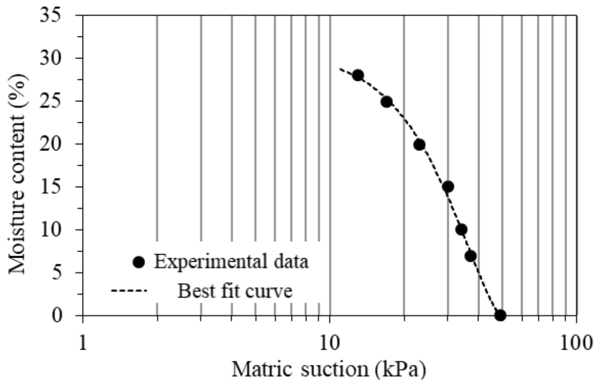

Fig. 2 Soil water characteristic curve of test material

Fig. 2 shows the soil water characteristic curve (SWCC) for DL clay. In order to draw SWCC, several specimens made up of test soil with varying water content were prepared and the value of initial matric suction was monitored. The procedure was adopted from the study performed by Farooq *et al.* (2004). The SWCC curve in the Figure initially showed a non-linear behavior followed by the linear behavior indicating that the soil suction increases with a decrease in moisture content.

Homogenous specimens were prepared by compacting

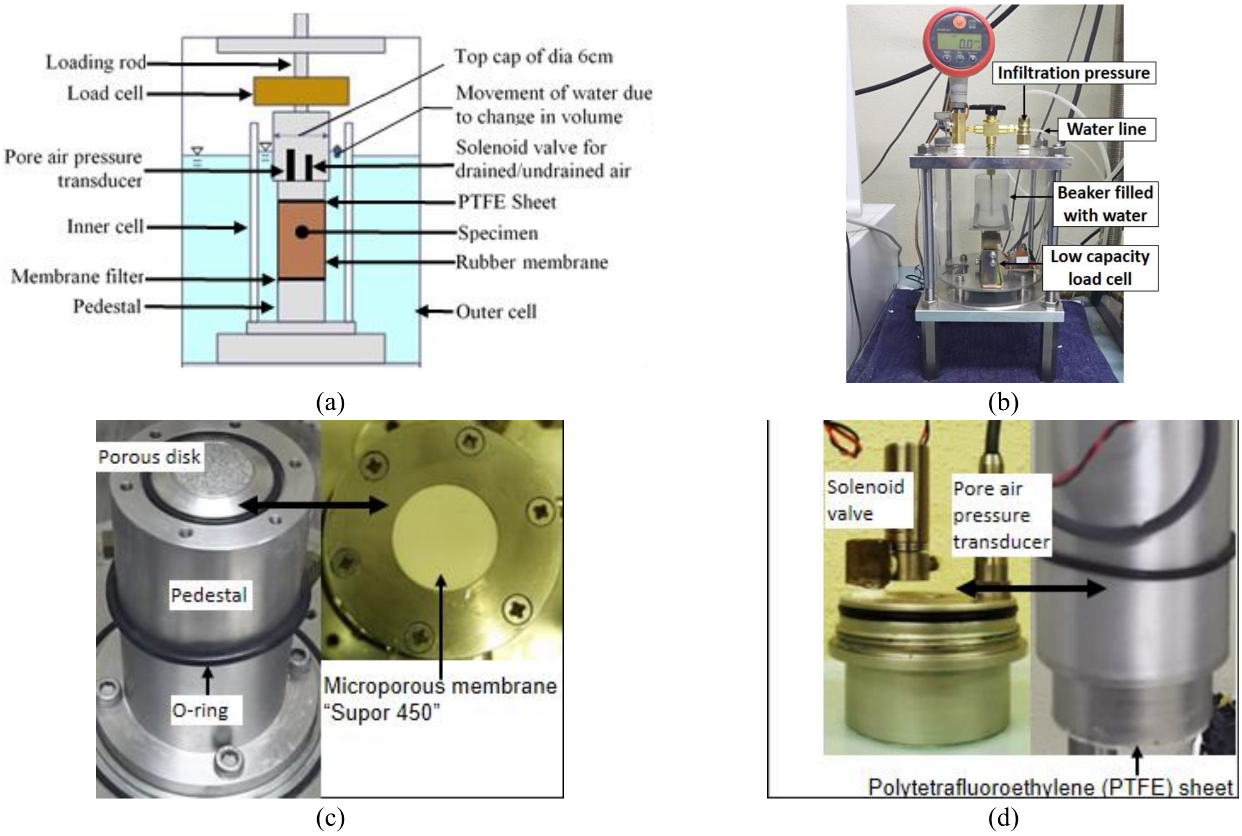

Fig. 3 Triaxial test apparatus (a) Double cell system, (b) External load cell, (b) Bottom pedestal & (d) Top cap

soil in 5 layers, each layer being 2 cm thick, with a static compaction machine with a hydraulic jack (Rasool and Kuwano 2018). The low energy from the static compaction can produce a uniform density throughout the length to prevent the development of a weaker region in the specimen (Meilani *et al.* 2005, Rahardjo *et al.* 2004). Before compaction, water was added to the dry DL clay to prepare soil samples at water content of 25% i.e. on the wet side of optimum water content. The specimens had a constant void ratio of 1.125 and a density of 1.24g/cm3 at degree of saturation (Sr) of 59.0%. The degree of compaction of all specimens was maintained at 80%. The pressure applied to the soil at the time of sample preparation was higher than the applied stresses during the test phase and hence the samples are considered over-consolidated. According to Nishimura *et al.* 1999, unsaturated soils that exist nearby ground surface and soils compressed manually are generally over-consolidated due to environmental changes.

2.2 Description of the test apparatus

During the rainfall, decrease in matric suction due to water infiltration on a soil slope causes a decrease in the mean effective stress which takes place under constant total stress and increasing pore water pressure conditions. The increase in pore water pressure is achieved by injecting water into triaxial specimen (Irfan & Uchimura 2015 and Farooq *et al.* 2004). The equipment used was an advanced strain-controlled triaxial apparatus suitable for unsaturated soil testing. It includes a double-walled triaxial cell, an axial loading device, pore-air, pore water and cell pressure and volume change measuring devices, and a suitable computer program for controlling test sequence and recording test data, as shown in Fig. 3(a). The confining pressure was applied on the top of a double cell chamber filled with the water by controlling the air pressure with a regulator. Supre precision regulator (RS/RR series) made by Fujikura Inc. Japan has a high accuracy of keeping the air pressure and hence the cell pressure was kept constant throughout the shear process. The volume of soil samples was measured by a Low Capacity Differential Pressure Transducer (LCDPT). The LCDPT measures specimen volume change as the variation in the water level in the inner cell. The change in water level was recorded by a computer, which was then calculated as the total volume change of specimen as per relations given in Japanese Geotechnical Society standard JGS0527-2009. The vertical deformation of the specimen was measured by a Linear Variable Differential Transformer (LVDT). In order to separate the routes for the measurement and the control of pore air and pore water pressure, a membrane filter and a PTFE (polytetrafluoroethylene, known as Teflon) sheet were used. The PTFE sheet was placed on the top of the specimen to cut off the flow of water and to control the air pressure, shown in Fig. 3 (d). The membrane filter was placed on a bottom pedestal to cut off the flow of air, as shown in Fig. 3(c). The thin membrane type "Supor 450" from Pall Corporation has pore size of 0.45 µm, member thickness of 140 µm and provided air entry value of 250 kPa. The same membrane has been used by Habasimbi & Nishimura (2019) and Nishimura

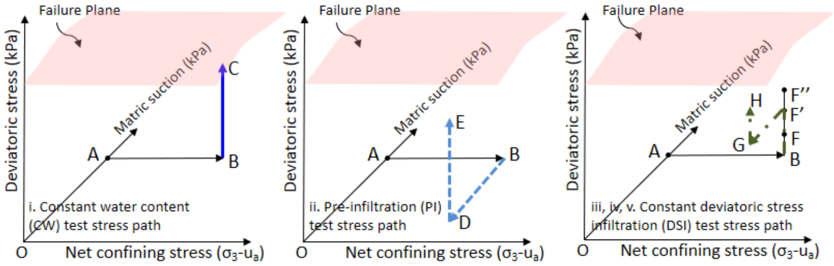

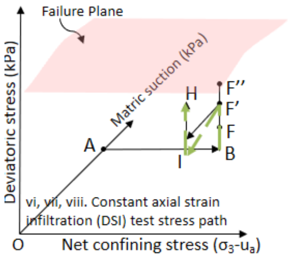

Sr. No.	TEST ID	STRESS PATH
i.	CW	A→B→C
ii.	PI	A→B→D→E
iii.	DSI25	A→B→F→G→H
iv.	DSI50	A→B→F'→G→H
v.	DSI75	A→B→F''→G→H
vi.	ASI25	A→B→F→I→H
vii.	ASI50	A→B→F'→I→H
viii.	ASI75	A→B→F''→I→H

Fig. 4 Loading history associated with the triaxial test program

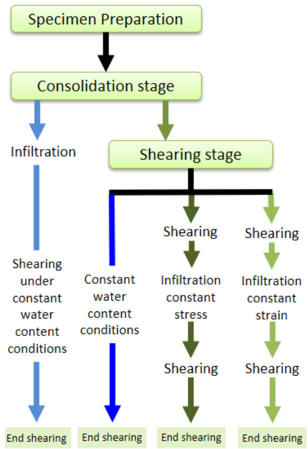

Fig. 5 Steps of the test program

(2014). Before the start of each experiment, a vacuum pressure of -101.3 kPa was applied to porous disk fitted on a base pedestal for removing air from the water line connecting porous disk and pore water pressure transducer. Water in an unsaturated soil specimen was infiltrated from the bottom pedestal which was connected to the beaker and pore water pressure transducer through the water line. Beaker was fitted on an external load cell placed in a cylindrical cell with a top cap closed, as shown in Fig. 3(b). The rate of infiltration was controlled by regulating the infiltration pressure applied on top of an external load cell. The infiltration pressure was increased in steps in order to ensure uniform distribution of water throughout the height of the specimen.

2.3 Stress state variables

The behavior of a soil can be described in terms of the state of stress in the soil (Nishigata *et al.* 2003). Terzaghi (1936) described the stress state variable controlling the behavior of saturated soil. The stress state variable for a saturated soil has been called the effective stress and is commonly expressed in the form of an equation:

$$\sigma' = \sigma - u_w \tag{1}$$

where, σ' = effective normal stress, σ = total normal stress and u_w = pore-water pressure

Due to the presence of air the above equation cannot be used to describe the behavior of unsaturated soils. Therefore, Bishop (1960) suggested a tentative expression for effective stress which has gained widespread reference.

$$\sigma' = (\sigma - u_a) - \chi(u_a - u_w) \tag{2}$$

where, u_a = pore-air pressure, χ = Parameter related to degree of saturation, $(\sigma - u_a)$ = net stress, $\chi(u_a - u_w)$ = suction stress

The current research also used two stress state variables i.e. $(\sigma - u_a)$ net stress and $(u_a - u_w)$ matric suction to define shear strength and deformation behavior of unsaturated soils.

2.4 Test procedure

After preparation, the specimens were put on a saturated pedestal and initial suction was measured after that cell pressure and pore air pressure was increased using the axis translation technique. As this research focused more on the behavior of shallow slopes, therefore, the pore air pressure was drained and controlled throughout the experimental process, whereas, pore water pressure was undrained except during water infiltration process. The water infiltration increased the pore water pressure only. A similar assumption was also made in the tests by Farooq *et al.* (2004) and Brenner *et al.* (1985). Specimens were consolidated at a net confining pressure of 100 kPa for approximately 20 hrs. after which shearing and water infiltration was carried out. Point B in Fig. 4 represents the point when the soil has a certain value of matric suction under a zero vertical load (i.e. zero deviatoric stress). The loading history associated with the triaxial test program and the flow chart of the whole experimental series is shown in Fig. 4 & Fig. 5. There are four criteria used in the research.

i. In the first criterion, the soil was sheared under constant water content conditions by keeping the drainage valve for pore water pressure close until it fail. The drainage valve for pore air pressure was kept drained and controlled throughout the test. As no water was infiltrated throughout the test process, therefore, it is known as constant water constant (CW) test. *BC* represents the path for the constant water content test.

ii. In the second criterion, water was infiltrated into the specimen right after isotropic consolidation by keeping constant deviatoric stress at 0 kPa, and then shear stress was applied. During the shearing process, drainage valve for both pore air and pore water pressure were kept open. This test is called as pre-infiltration (PI) test. *BD* shows the path when matric suction was decreased to start water infiltration. *DE* shows the path when the soil was sheared after completion of the water infiltration process.

iii. In the third criterion, the shear stress was applied after isotropic consolidation and water was infiltrated into the specimen when a certain level of deviatoric stress was achieved by keeping this value of deviatoric stress constant. The specimen was sheared again after the water is being infiltrated to achieve the required degree of saturation. This test is called as constant deviatoric stress infiltration (DSI) test.

iv. In the fourth criterion, the shear stress was applied after isotropic consolidation and water was infiltrated into the specimen when a certain level of axial strain was achieved by keeping the value of axial strain constant. The specimen was sheared again after water is being infiltrated to achieve the required degree of saturation. This test is called a constant axial strain infiltration (ASI) test.

Normally, shear strength parameters are obtained from test samples that have been infiltrated with water before the shear test. In particular, it is meaningless to use shear strength parameters in which water has been infiltrated previously and collapse has already occurred, because the collapse due to water infiltration is a discontinuous phenomenon in soil skeleton. This method did not sufficiently express the actual condition of the slopes. A more realistic approach to obtain shear strength of unsaturated soil is to infiltrate water under shear stress conditions. Therefore, the constant deviatoric stress and constant axial strain tests in this research are performed to simulate the actual condition of slope through the triaxial test series. These tests also give an idea whether the shear strength under water infiltration conditions remains similar to shear stress under a constant water content condition. The constant deviatoric stress infiltration tests and constant axial strain infiltration tests can also be designated as shearing-infiltration tests. The shearing-infiltration tests in Sr. No. 3 & 4 have been carried in two stages. In the first stage, shearing was carried out in constant water content conditions by keeping the drainage valve for pore water pressure closed. The valve was opened during the water infiltration process and once the water is infiltrated to achieve the required degree of saturation. The second shearing was carried out by keeping the valve for pore water pressure closed. The drainage valve for pore air pressure was kept drained and controlled throughout the test. The shearing-infiltration tests were conducted at different constant deviatoric stress and axial strain levels. F, F' and F" in Fig. 4 represents 25%, 50% and 75% of maximum deviatoric stress and axial strain level at which water infiltration was carried out. *FG* is the wetting path which shows a decrease in matric suction due to water infiltration., whereas, *GH* is second shearing after completion of the water infiltration process.

2.5 Test conditions with respect to water infiltration

This research has been performed considering two cases, (a) in Case-I ≈20 cm^3 of water was infiltrated to increase degree of saturation about 88%, (b) in Case-II ≈10 cm^3 of water was infiltrated to increase the degree of saturation about 78%. 88% degree of saturation is the maximum degree of saturation of studied soil. Thus, Case-I represents the field condition when the soil achieved its maximum degree of saturation. In Case-II, 78% degree of saturation represents the field condition when the soil is still not fully saturated. The results of the effect of loading states, infiltration pressure on infiltration rate and deformation behavior of Case-I are presented here because specimens in Case-II have shown the same behavior. The stress-strain behavior and unique stress-strain curves for both cases are presented. The nomenclature used in Figures is e.g. 1ASI25 etc. Where, "1" represents the test case "Case-1". "ASI" is for "Constant axial strain infiltration test". "25" is for "Constant axial strain of 25%".

2.6 Loading states

The purpose of this research is to investigate the shear strength and deformation behavior of unsaturated soil under water infiltration at different loading states. In order to perform the test with different loading states, the loading system of the triaxial test apparatus was found capable of maintaining constant axial stress and axial strain for a long duration of time with good accuracy. The loading system was connected to a computer and controlled by a custom-built software. The procedure of loading applied during the constant stress test is as follows. First, the loading system was operated by strain-controlled method up to the required deviatoric stress level. When the required deviatoric stress level reached, the apparatus was switched to stress controlled method and the water was infiltrated into the specimen. After the completion of the water infiltration process, the loading system was switched to strain-

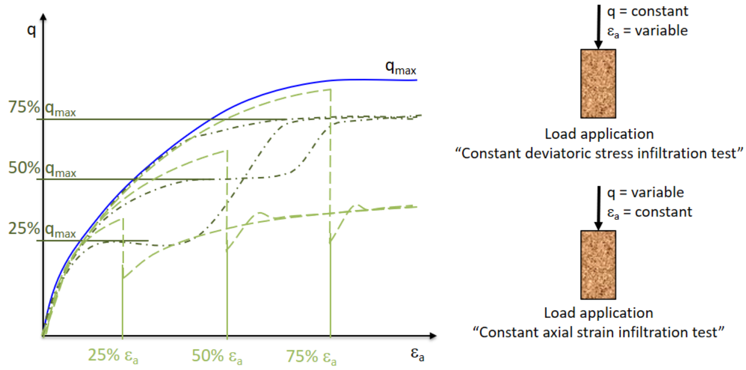

Fig. 6 Tentative stress-strain curve

controlled method again. Three types of deviatoric stress axial and strain level considering low, medium and high were used, the details of different loading states implemented in this study are explained below,

i. **Constant water content (CW) test:** This is a simple shear test in which water content remained the same throughout the test. Maximum deviatoric stress (q_{max}) was obtained from this test. The tentative curve of constant water content test is shown in Fig. 6.

ii. **Pre-infiltration (PI) test:** In this test, water infiltration was carried out at zero deviatoric stress (q = 0 kPa)

iii. **Constant deviatoric stress infiltration (DSI) test:** The deviatoric stress level at the time of water infiltration is defined by the following equations.

$$\text{DSI} = \frac{(\sigma_1 - \sigma_3)_I}{(\sigma_1 - \sigma_3)_{max}} x100 \tag{3}$$

where, $(\sigma_1 - \sigma_3)_I$ is deviatoric stress at the time of water infiltration and $(\sigma_1 - \sigma_3)_{max}$ is the maximum deviatoric stress from the constant water content test. In this research, three deviatoric stress levels of 25%, 50%, and 75% of q_{max} have been used. The tentative curves for three levels of deviatoric stress are shown in Fig. 6.

iv. **Constant axial strain infiltration (ASI) test:** The axial strain level at the time of water infiltration is defined by the following equations.

$$\text{ASI} = \frac{(\varepsilon_a)_I}{(\varepsilon_a)_{max}} x100 \tag{4}$$

where, $(\varepsilon_a)_I$ is the axial strain at the time of water infiltration and $(\varepsilon_a)_{max}$ is the maximum axial strain. This research is performed according to the Japanese Geotechnical Society Standard "JGS 0527-1998 Method for Triaxial Compression Test on Unsaturated Soils", the value of maximum axial strain is taken from the same standard. In this research, three axial strain levels of 25%, 50% and 75% of $(\varepsilon_a)_{max}$ has been used. The tentative curves for three levels of axial strain are shown in Fig. 6.

3. Experimental results

3.1 Effect of loading state on water infiltration

Fig. 7 illustrates the effect of loading states on axial deformation during the course of water infiltration. Less axial deformation was observed in the specimen in the pre-infiltration test as shown in Fig. 7(a), because the water infiltration was carried out at constant zero deviatoric stress. Fig 7(b) shows the results of constant shear stress infiltration tests. It can be seen that axial deformation increased with an increase in deviatoric stress level. The specimen 1DSI75 showed maximum axial deformations. Specimen 1DSI75 was first sheared to deviatoric stress of 75% q_{max} in undrained conditions which results in the development of pore water pressure inside the specimen. When the pore water pressure valve was opened, initially some water drained out of specimen, as shown by "X". The water infiltration was carried out by increasing infiltration pressure in steps until the required degree of saturation is achieved. The results of constant axial strain infiltration tests are shown in Fig 7(c). It can be seen that as axial strain was kept constant, no increase in axial strain was observed during the water infiltration process. The test results showed that axial deformation occurred when deviatoric stress was kept constant, whereas, no axial deformation occurred when the axial strain was kept constant during the course of water infiltration, this also verified constant loading states phenomenon.

3.2 Effect of infiltration pressure on water infiltration rate

Fig. 8 shows the effect of infiltration pressure on water infiltration. Fig. 8(a) shows the results of the pre-infiltration test. Fig 8(b) shows the results of constant deviatoric stress infiltration tests and Fig. 8(c) shows the results of constant axial strain infiltration tests. The loading system was controlled by a computer to maintain constant deviatoric stress and constant axial strain throughout the water infiltration process. In all cases ≈20 cm^3 water was infiltrated into the specimens to achieve ≈88% degree of saturation. The infiltration pressure was increased in steps of the one-hour interval. It can be seen that water infiltration increased with an increase in infiltration pressure. It was also observed that carrying out water infiltration in steps helped in the uniform distribution of water throughout the height of the specimen. The uniform distribution of water in the specimen was observed by

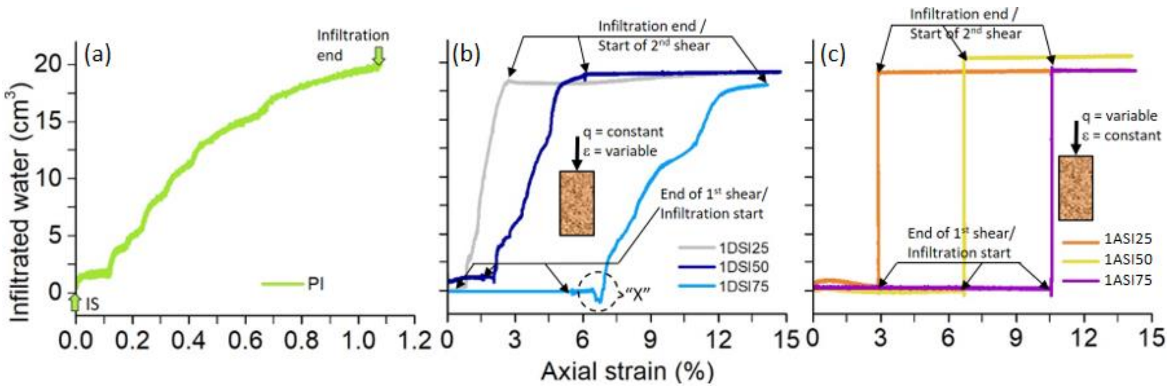

Fig. 7 Effect of different loading states

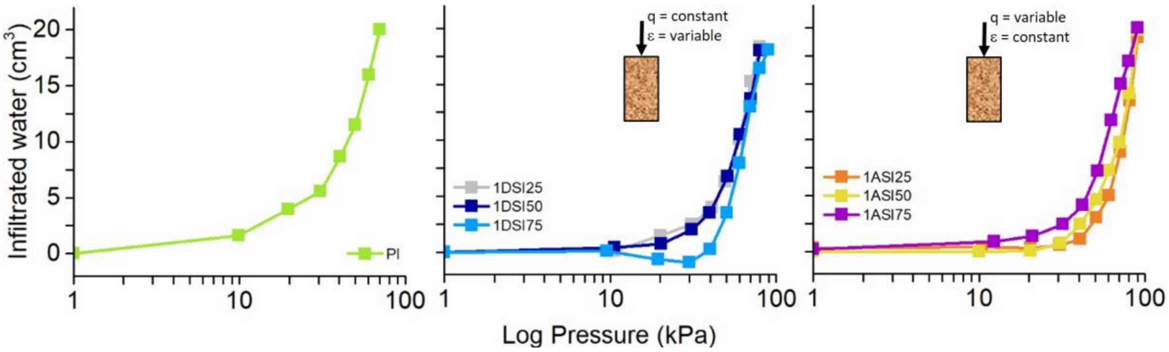

Fig. 8 Effect of infiltration pressure on water infiltration

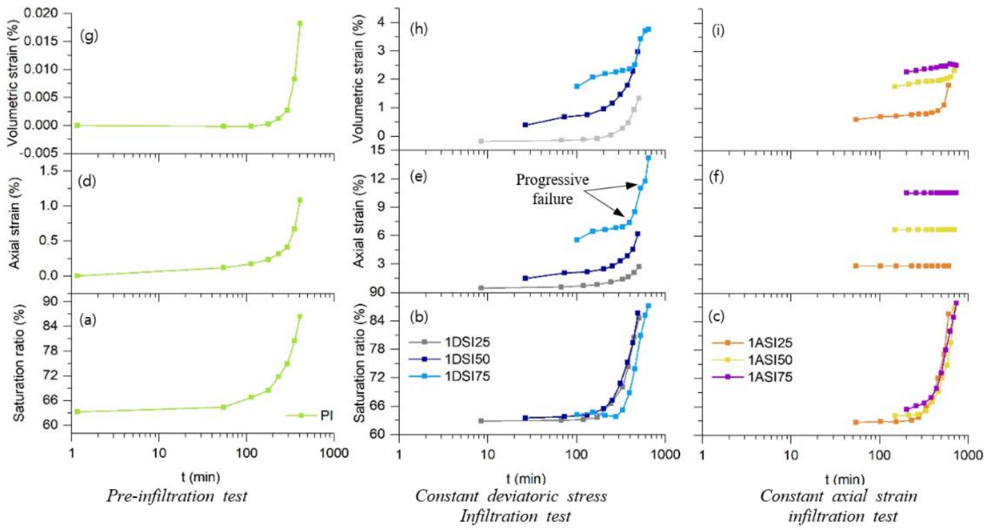

Fig. 9 Deformation behavior during water infiltration

cutting the specimen at the end of the test by measuring moisture content in the specimen.

3.3 Deformation behavior during water infiltration

The slope failures caused by rainfall is directly related to the rainfall intensity in a specific area. It is not necessary that all rain-water infiltrated into the soil, some portion of water did not penetrate and flow as surface run-off. A better parameter to measure deformations is the volume of water infiltrating into the soil. It shows a more direct relation between soil degree of saturation and deformation (Farooq *et al.* 2004). The deformation behavior of soil in terms of degree of saturation, axial and volumetric strain during the course of water infiltration is shown in Fig. 9. Fig. 9(a, b, c) shows an increase in degree of saturation due to water infiltration. As the same volume of water was infiltrated in all specimen, therefore, the specimens have shown the same degree of saturation. The increase in axial strain during the course of water infiltration is shown in Fig. 9(d,e,f). In the pre-infiltration test, water was infiltrated at constant deviatoric stress of 0 kPa and axial deformations observed was 1.1%. In constant deviatoric stress infiltration tests, water was infiltrated at constant deviatoric stress 25%, 50%, and 75% of q_{max} and axial deformations increased with increase in deviatoric stress level. In both test series, there was a continuous development of axial strain during the process of water infiltration without the application of further deviatoric stress. A possible explanation for this deformation response was that during the phase of water infiltration bond between the soil grains broken as water permeate through the pores, resulting in continuous deformation. The specimen 1DSI75 showed a rapid increase in axial strain at 70% degree of saturation corresponds to 7.5% axial strain. The increase in axial strain depicts the initiation of local failure within the specimen, the increase in axial strain continued with water infiltration and ultimately the progressive failure occurred at 86% degree of saturation corresponds to 12% axial strain. This failure was identified when the water started to come out of the drainage pipe at the top of the specimen. According to Darban *et al.* (2019), the process which brings the slope to final collapse starts with local soil failure, which then leads to formation and propagation of a shear zone, and finally to general slope failure. This mechanical process is called progressive failure. No axial deformation was observed in constant axial strain infiltration tests as axial strain was kept constant during the course of water infiltration as shown in Fig. 9(f). The change in volumetric strain is shown in Fig. 9(g, h, i). It can be seen that all specimens showed compressive behavior. In the case of the pre-infiltration test, less volume deformation occurred because no vertical load was applied during the course of water infiltration. In the case of infiltration under constant shear stress, axial deformation combined with the volume change result in more volume decrease. Whereas, in the case of constant axial strain infiltration tests, as no axial deformation occurred during water infiltration, therefore, specimens exhibit less decrease in volume.

3.4 Volume change behavior

In presenting the test results, the total volumetric strain, (ε_v) is a ratio between the total volume change and the initial volume of the specimen. Dilation of the specimen is expressed by negative total volumetric strain and compression is expressed by a positive total volumetric strain. Fig. 10 illustrates the relation between total volumetric strain versus axial strain for all test cases during the whole shearing process (including water infiltration). The result shows the decrease in volume of the specimen with an increase in axial strain. The results are in consistence with the study carried by Oka *et al.* 2010 on DL clay which stated that for the volumetric strain, the soil specimen exhibits contractancy during shearing and the volume continuously decreases. The results also indicate that except pre-infiltration test, the soil specimens showed the same volume change behavior before water infiltration as in the constant water content test. Fig. 10(a) shows the volume change behavior of pre-infiltration test, the specimen showed decrease in volume as compared to constant water constant test due to water infiltration. Fig. 10(b) shows the results of constant deviatoric stress infiltration tests. It can be seen that volumetric strain during water infiltration process, for specimens 1DSI25, 50, 75 was 2.6%, 2.5% and 2.1% respectively, which shows that volumetric strain decrease with increase in deviatoric stress level. As previously explained, the specimen 1DSI75 failed during the course of water infiltration at 12% axial strain, therefore, no further change in volume was observed in this specimen. Volume change behavior for constant axial strain infiltration tests is shown in Fig. 10(c). The volumetric strain during the water infiltration process for specimens 1ASI25, 50, 75 was 1.2%, 0.6% and 0.25% respectively, which shows that volumetric strain decrease with an increase in axial strain level. In DSI & ASI tests, the specimens were already sheared to 25%, 50% and 75% q_{max} and ε_{max}, up to these levels specimens had already undergone volume deformation due to shearing. Consequently, the decrease in volume deformations due to water infiltration was observed with an increase in the level of stress or strain. However, in ASI tests, as the axial strain was kept constant, therefore, the volumetric strain is due to change in the radial direction of specimen only and test results showed less volumetric strain as compared to constant deviatoric stress infiltration tests.

3.5 Shear strength behavior

The deviatoric stress (σ_1-σ_2) versus axial strain relationship for both cases is shown in Fig. 11. The figure shows the effect of water infiltration on the shear strength of unsaturated soil at different deviatoric stress and axial strain levels. The shearing in shear-infiltration tests was performed in two stages. In the first stage, specimens were sheared to a predefined level of deviatoric stress or axial stain in constant water content conditions. After that, water in specimens was infiltrated by keeping deviatoric stress/axial strain constant. Once the water was infiltrated to achieve the required degree of saturation, the specimens were sheared again in constant water content conditions. Fig. 11(a) shows the results of Case-I in which degree of saturation was increased to ≈88%. The maximum deviatoric stress was obtained from the constant water content test. In the pre-infiltration test, water was infiltrated at constant q=0kPa and some reduction in deviatoric stress was observed. The specimen 1DSI25 was first sheared to 25% of q_{max} and water was infiltrated by keeping the deviatoric stress constant and 2.3% axial strain was developed during the water infiltration process. The specimen was sheared again after completion of water infiltration and an increase in shear stress was observed until the end of the shearing process. The specimen 1DSI50 was sheared to 50% of q_{max} and water was infiltrated by keeping the deviatoric stress constant and 4.7% axial strain was developed during the water infiltration process. The specimen was sheared again after completion of water infiltration. During the second shearing, the deviatoric stress increased with an increase in axial strain and specimen failed at 11.5% axial strain after which no more increase in deviatoric stress was observed. The specimen 1DSI75 was sheared to 75% of q_{max} and water was infiltrated by keeping the deviatoric stress constant. However, in this specimen, a continuous increase in axial strain was observed during the course of water infiltration and specimen failed at 12% axial strain. It was also observed that once the failure occurs, the deviatoric

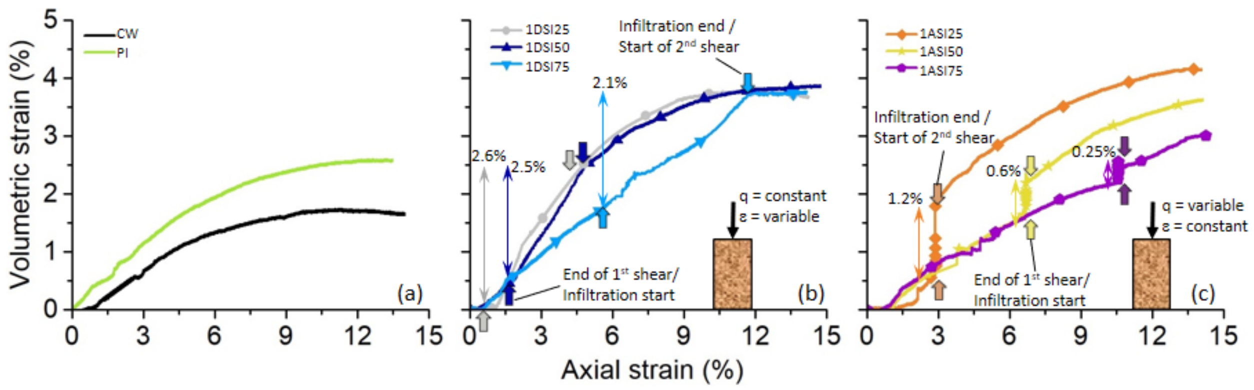

Fig. 10 Volume change behavior

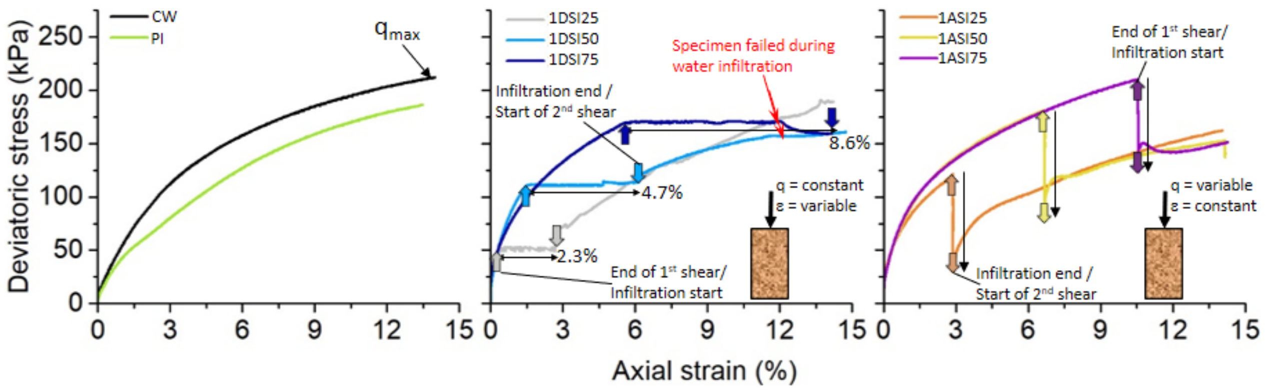

(a) Case-I

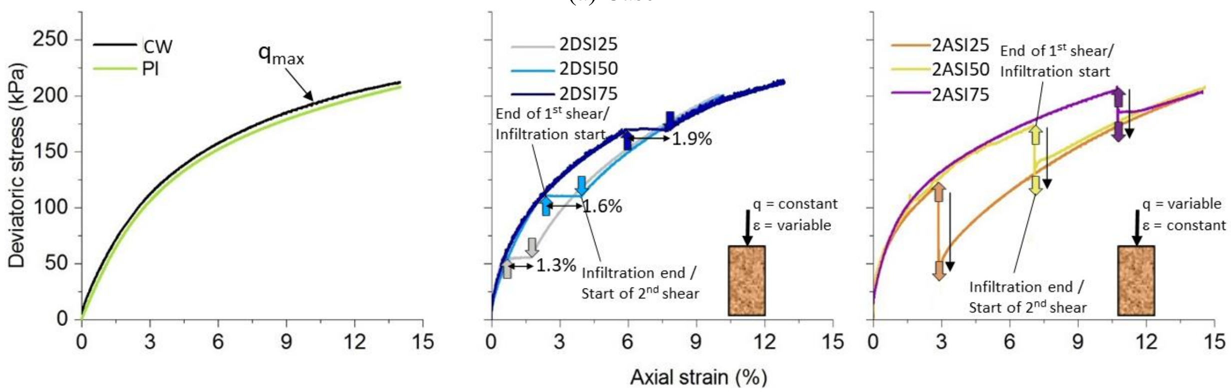

(b) Case-II

Fig. 11 Shear strength behavior (a) Case-1, 20 cm^3 water infiltrated (b) Case-II, 10 cm^3 water infiltrated

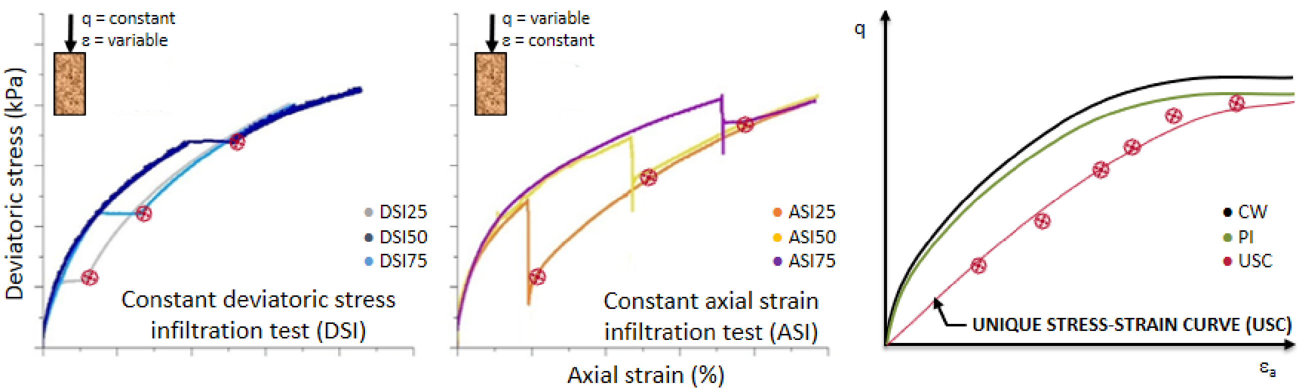

Fig. 12 General concept/schematic representation of the unique stress-strain curve

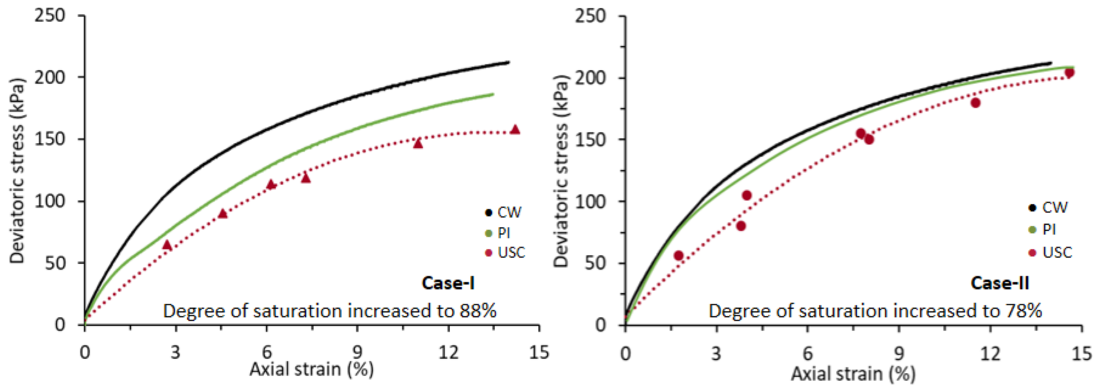

Fig. 13 Unique stress-strain curve

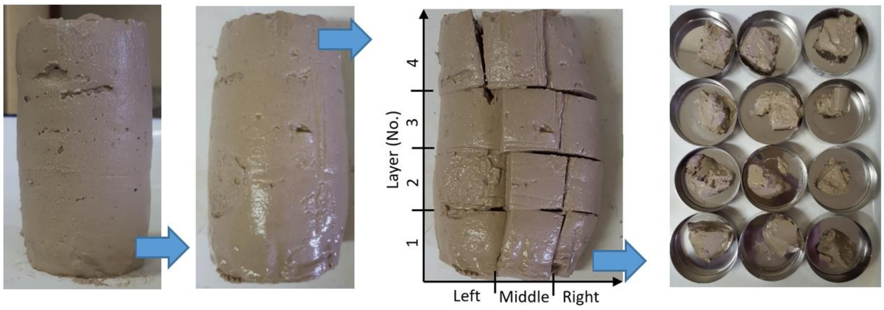

Fig. 14 Moisture distribution in specimen at the end of test

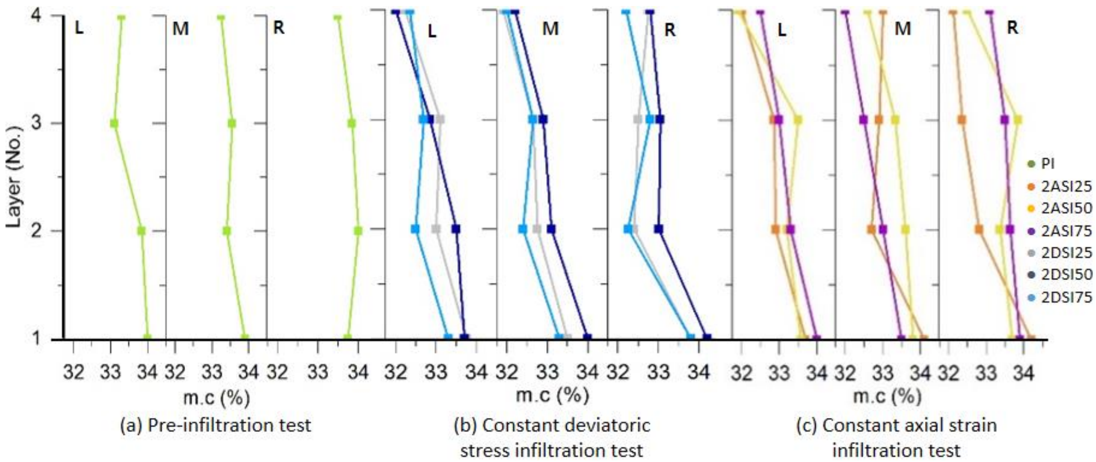

Fig. 15 Moisture distribution in specimen at the end of test

stress could no longer be maintained by the loading system and deviatoric stress decreased. This behavior was also observed by Farooq *et al.* (2004) and Irfan & Uchimura (2014).

The failure in specimen 1DSI50 & 1DSI75 was also identified by the dissipation of pore water in the specimen i.e., water started to come out from the drainage pipe at the top of the specimen. In shear-infiltration constant axial strain tests, as the axial strain was kept constant during the course of water infiltration, the deviatoric stress decreased to the lowest point. When the specimen was sheared after the completion of water infiltration, the deviatoric stress increased again with increase in axial strain. Increase in deviatoric was observed in specimens 1ASI25, 1ASI50 and 1ASI75 during second shearing. However, the specimen 1ASI50 and 1ASI75 failed at 11.5% and 12% axial strain respectively during the second shearing and no further increase in deviatoric stress was observed in these specimens. The failure was identified by the dissipation of pore water in the specimens i.e., water started to come out of the drainage pipe at the top of the specimen.

Fig. 11(b), shows the results of Case-II when the degree of saturation was increased to ≈78%. In constant deviatoric stress infiltration tests, the axial strain developed in specimens 1DSI25, 1DSI50 and 1DSI75 during the course of water infiltration was 1.3%, 1.6% and 1.9%. All the specimens showed an increase in deviatoric stress after completion of the water infiltration process. Similarly, in constant axial strain infiltration tests, deviatoric stress decreased during the course of water infiltration as axial strain was kept constant. However, all specimens showed an increase in deviatoric stress after completion of the water infiltration process. It was also noted that no decrease in deviatoric stress was observed in Case-II when the degree of saturation was increased ≈78%. Therefore, it can be said that the effect of water infiltration was more pronounced in specimens with a higher degree of saturation.

The failure in specimen 1DSI50 & 1DSI75 was also identified by the dissipation of pore water in the specimen i.e., water started to come out from the drainage pipe at the top of the specimen. In shear-infiltration constant axial strain tests, as the axial strain was kept constant during the course of water infiltration, the deviatoric stress decreased to the lowest point. When the specimen was sheared after the completion of water infiltration, the deviatoric stress increased again with increase in axial strain. Increase in deviatoric was observed in specimens 1ASI25, 1ASI50 and 1ASI75 during second shearing. However, the specimen 1ASI50 and 1ASI75 failed at 11.5% and 12% axial strain respectively during the second shearing and no further increase in deviatoric stress was observed in these specimens. The failure was identified by the dissipation of pore water in the specimens i.e., water started to come out of the drainage pipe at the top of the specimen.

Fig. 11(b), shows the results of Case-II when the degree of saturation was increased to ≈78%. In constant deviatoric stress infiltration tests, the axial strain developed in specimens 1DSI25, 1DSI50 and 1DSI75 during the course of water infiltration was 1.3%, 1.6% and 1.9%. All the specimens showed an increase in deviatoric stress after completion of the water infiltration process. Similarly, in constant axial strain infiltration tests, deviatoric stress decreased during the course of water infiltration as axial strain was kept constant. However, all specimens showed an increase in deviatoric stress after completion of the water infiltration process. It was also noted that no decrease in deviatoric stress was observed in Case-II when the degree of saturation was increased ≈78%. Therefore, it can be said that the effect of water infiltration was more pronounced in specimens with a higher degree of saturation.

3.6 Unique stress-strain curve

The deviatoric stress vs. axial strain relationship shows that the specimens in the respective test series followed the same shear stress path after water infiltration. Therefore, the curve is drawn by joining the points to show the same stress path is known as unique stress-strain curve. The unique stress-strain curve also called as the characteristic curve at water infiltrated can be drawn if an same volume of water is infiltrated in specimens. A unique stress-strain curve is drawn by taking the final strain stop point in stress-controlled test and the lowest point of deviatoric stress just after a peak during the second shearing in strain-controlled. The general concept of the unique infiltration curve is drawn in Fig. 12.

Fig. 13 shows the unique stress-strain curve for both Cases. It can be seen that a unique stress-strain curve exists on the lower side of the stress-strain curve for constant water content test and pre-infiltration test. Hence, show a reduction in deviatoric stress of soil due to water. It shows that under the same net stress if an equal amount of water is infiltrated, the specimens will follow the same path after infiltration. The curve represents the stress-strain relationship that expresses the transient situation from unsaturated condition to failure state due to water infiltration for the specimens with a higher degree of saturation. The unique stress-strain curve also shows that shear strength of unsaturated soil under water infiltration conditions is independent of deviatoric stress level on soil.

3.7 Variation of moisture content at the end of test

In order to facilitate the uniform distribution of water throughout the height of the specimen, water was infiltrated from the bottom pedestal having a thin membrane filter with pores of 0.45 μm by applying the infiltration pressure. The infiltration pressure was applied at the top of the external cylindrical chamber having beaker placed on a load cell (Fig. 3(c)) and was increased in steps of the one-hour interval. It took approximately 9 hours to complete the water infiltration process. The uniform distribution of water along the height of the specimen at the end of each test was measured by cutting the specimen in three vertical and four horizontal sections. Fig. 14 shows the moisture distribution in the specimen at the end of the test in Case-I in which 20 cm^3 of water was infiltrated to achieve 88% degree of saturation which is the maximum degree of saturation for studied soil. So the sample is said to have its maximum degree of saturation. The cut samples were then oven-dried for one day and water content was measured and shown in Fig. 15. Fig. 15((a), (b), (c)) shows the gravimetric water content measured along the height of the specimen in the pre-infiltration test, constant deviatoric stress infiltration test and constant axial strain infiltration test, respectively, in Case-I. It can be seen that water content varied a little bit along the height of the specimen. Since no filter paper or any other material was used around the specimen, the water content at the base of the specimen was observed higher than at the top, but this difference is within 1.5%. This shows that the technique of infiltrating water by increasing the infiltration pressure of one-hour interval was satisfactory for the uniform distribution of water along the height of specimens.

4. Conclusions

A series of laboratory element tests were conducted to examine the behavior of unsaturated soil that was subjected to water infiltration under different loading states. The following conclusions can be drawn from the study:

The deviatoric stress remains unchanged in the constant deviatoric stress test, whereas, axial strain remains unchanged constant axial strain test. This shows that any kind of loading can be applied to study the behavior of the soil.

The shear strength of the soil is not much affected at less water infiltration, whereas, it is affected by more water infiltration and at a high level of deviatoric stress water infiltration alone can induce failure in the soil without having to have any additional loading.

In most cases, the soil is not failed due to water infiltration but deforms in all cases and deformation varied for different levels of deviatoric stress and axial strain.

The unique stress-strain curve shows that if the same amount of water is infiltrated into the specimens they will follow the same path after water infiltration. It also shows that reduction in shear strength of the soil due to water infiltration can be calculated by performing the test at any deviatoric stress level on the soil.

Finally, it can be said that the water infiltration causes a change in volumetric strain and degree of saturation of unsaturated soil which results in significant deformation. As a result, even if the soil is not failed the significant deformation may hinder the function of soil structures, therefore, the deformations should be considered while analyzing soil behavior due to water infiltration.

Acknowledgments

The Saitama University Japan and Japanese Ministry of Education, Culture, Sports, Science and Technology (MEXT) is gratefully acknowledged for research facilities and financial assistance.

References

Bishop, A.W. (1960), "The measurement of pore pressure in the triaxial test", *Proceedings of the Conference on Pore Pressure and Suction in Soils*, London, U.K.

Brenner, R.P., Tam, K.H. and Brnad, E.W. (1985), "Field stress path simulation of rain-induced slope failure", Proceedings of the 11th International Conference on Soil Mechanics and Foundation Engineering, San Francisco, California, U.S.A., August.

Darban, R., Damiano, E., Minardo, A., Olivares, L., Picarelli, L. and Zeni, L. (2019), "An experimental investigation on the progressive failure of unsaturated granular slopes", *Geosciences*, **9**(2), 63. https://doi.org/10.3390/geosciences9020063.

Fredlund, D.G., Rahardjo, H., Fredlund, M.D. (2012), *Unsaturated Soil Mechanics in Engineering Practice*, John Wiley and Sons, New York, U.S.A.

Farooq, K., Orense, R. and Towhata, I. (2004), "Response of unsaturated sandy soils under constant shear stress drained condition", *Soils Found*., **44**(2), 1-13. https://doi.org/10.3208/sandf.44.2_1.

Gui, M.W. and Wu, Y.M. (2014), "Failure of soil under water infiltration condition", *Eng. Geol*., **181**(1), 124-141. https://doi.org/10.1016/j.enggeo.2014.07.005.

Habasimbi, P. and Nishimura, T. (2019), "Soil water characteristic curve of an unsaturated soil under low matric suction ranges and different stress conditions", *Int. J. Geosci*., **10**, 39-56. https://doi.org/10.4236/ijg.2019.101004.

Ifran, M. and Uchimura, T. (2015), "Helical filter paper technique for uniform distribution of injected moisture in unsaturated triaxial specimens", *Soils Found*., **55**(4), 749-760. https://doi.org/10.1016/j.sandf.2015.06.008.

JGS 0527-2009 (2009), "Method for triaxial compression test on unsaturated soils (Standards of Japanese Geotechnical Society)", Japanese Geotechnical Society, Tokyo, Japan.

Kato, S. and Kawai, K. (2000), "Deformation characteristics of a compacted clay in collapse under isotropic and triaxial test state", *Soils Found*., **40**(50), 75-90. https://doi.org/10.3208/sandf.40.5_75.

Kim, Y. and Jeong, S. (2017), "Modeling of shallow landslides in an unsaturated soil slope using a coupled model", *Geomech. Eng*., **13**(2), 353-370. https://doi.org/10.12989/gae.2017.13.2.353.

Kim, Y., Rahardjo, H. and Satyanaga, A. (2018), "Numerical simulations of triaxial shearing-infiltration tests", *Soils Found*., **58**(2), 389-411. https://doi.org/10.1016/j.sandf.2018.02.009.

Mahmood, K., Kim, J.M. and Ashraf, M. (2016), "The effect of soil type on matric suction and stability of unsaturated slope under uniform rainfall", *KSCE J. Civ. Eng*., **20**(4), 1294-1299. https://doi.org/10.1007/s12205-015-0796-z.

Melinda, F., Rahardjo, H., Han, K.K. and Leong, E.C. (2004), "Shear strength of compacted soil under infiltration conditions", *J. Geotech. Eng*., **130**(8), 807-817. https://doi.org/10.1061/(ASCE)1090-0241(2004)130:8(807).

Meilani, I., Rahardjo, H. and Leong, E.C. (2005), "Pore-water pressure and water volume change of an unsaturated soil under infiltration conditions", *Can. Geotech. J*., **42**(6), 1509-1531. https://doi.org/10.1139/t05-066.

Nishimura, T., Hirabayashi, Y., Fredlund, D.G. and Gan, J.K. (1999), "Influence of stress history on the strength parameters of an unsaturated statically compacted soil", *Can. Geotech. J*., **36**(2), 251-261. https://doi.org/10.1139/cgj-36-2-251.

Nishimura, T. (2014), "Influence of seepage event on cyclic triaxial behavior of a compacted unsaturated soil", *Proceedings of the 6th International Conference on Unsaturated Soils*, Sydney, Australia, July.

Nishigata, T., Nishida, K. and Araki, S. (2003), "Behavior of unsaturated decomposed granite soil during water infiltration", *Proceedings of the 3rd International Conference on Unsaturated Soils*, Recife, Brazil, March.

Oka, F., Kodaka, T., Suzuki, H., Kim, Y.S., Nishimatsu, N. and Kimoto, S. (2010), "Experimental study on the behavior of unsaturated compacted silt under triaxial compression", *Soils Found*., **50**(1), 27-44. https://doi.org/10.3208/sandf.50.27.

Pirone, M., Papa, R., Nicotera, M.V. and Urciuoli, G. (2015), "In situ monitoring of the groundwater field in an unsaturated pyroclastic slope for slope stability evaluation", *Landslides*, **12**(2), 259-276. https://doi.org/10.1007/s10346-014-0483-z.

Rahardjo, H., Ong, B.H. and Leong, E.C. (2004), "Shear strength of a compacted residual soil from consolidated drained and constant water content triaxial tests", *Can. Geotech. J*., **41**(3), 421-436. https://doi.org/10.1139/t03-093.

Rasool, A.M. and Kuwano. J. (2018), "Influence of matric suction on instability of unsaturated silty soil in unconfined conditions", *Int. J. GEOMATE*, **14**(42), 1-7. https://doi.org/10.21660/2018.42.7115.

Sorbino, G. and Nicotera, M.V. (2013), "Unsaturated soil mechanics in rainfall-induced flow landslides", *Eng. Geol*., **165**, 105-132. https://doi.org/10.1016/j.enggeo.2012.10.008.

CC